

**AN EXPERIMENTAL AND NUMERICAL STUDY  
ON THE ENERGY ABSORBING  
CAPABILITY OF ALUMINUM EXTRUSIONS UNDER  
OBLIQUE LOADING**

*A. Reyes, M. Langseth and O. S. Hopperstad  
Structural Impact Laboratory - SIMLab  
Department of Structural Engineering  
Norwegian University of Science and Technology  
Rich. Birkelandsvei 1a, N-7491 Trondheim, Norway  
e-mail: aase.reyes@bygg.ntnu.no*

## Abstract

Oblique loading was studied through static experiments and numerical simulations. The behavior of square aluminum columns in alloy AA6060 subjected to oblique loading was investigated experimentally for three different load angles. The square columns were clamped at one end and oblique load conditions were realized by applying a force with different angles to the centerline of the column. Numerical simulations were later carried out to validate the numerical model.

## 1 Introduction

Lightweight materials such as aluminum alloys are attractive in the automotive industry because of the environmental advantages a lighter vehicle gives. Weight savings of 25% can be achieved when using aluminum instead of conventional steel structures. This will reduce fuel consumption and lower emission of carbon dioxide.

Energy absorbers are often used in vehicles to protect passengers and the structure itself during impact. For low speed impacts, the axial energy absorption mechanism has been implemented by placing energy absorbers in the front and the rear end of the body structure. These energy absorbers are called crash boxes and are designed to control the initial kinetic energy of the car during impact, while the force levels are kept sufficiently low to avoid permanent deformations in the rest of the car body. The absorption of energy is controlled by plastic work in the crash box, which is directly given from the area under the force-displacement curve.

Although the crash box elements can absorb all the kinetic energy of the vehicle during a low-speed crash, a high-speed crash will activate a larger part of the structure in order to absorb all the energy. When the crash boxes are fully deformed, the deformations are transferred to the front rail and subsequently to the rest of the vehicle's structure. This may lead to both bending and axial loading of other structural parts. Analytical studies of both pure bending [1] and axial crushing of square columns [2] have been completed over many years, resulting in expressions for mean forces and bending moments.

During an actual crash event, the energy absorber will seldom be subjected to either pure axial or bending collapse, but rather a combination of the two modes. The automotive industry requires that the bumper system must endure a load with an angle of 30 degrees to the longitudinal axis. The crash boxes will be subjected to both axial forces and moments in an oblique crash. If the crash box experiences global bending instead of axial crushing, the energy absorption will be lower, and both moments and axial forces will be transferred to the rest of the structure. It is therefore important to understand what happens to the crash box when subjected to oblique impact. Studies in this area are limited, but Han and Park [3] have investigated columns of mild steel subjected to oblique loading numerically. They obtained oblique conditions by impacting the column at a declined rigid wall with no friction. The response was divided into axial collapse, bending collapse and a transition zone, and an empirical expression for the critical angle was found.

In this paper, the behavior of square aluminum columns subjected to oblique loading is investigated. The objective of this study on oblique-loaded specimens has been (1) to build a test rig for accurate measurements of the quasi-static response; (2) to determine the characteristics of the collapse modes; and (3) to examine the energy absorbing capability. In total, 18 static tests were carried out to validate a numerical model and get some insight into the behavior of aluminum columns subjected to oblique loading.

## 2 Terminology

Figure 1 shows how oblique loading was realized for the experiments and the numerical analyses. The column was clamped at the lower end, and the force,  $F$ , was applied through a rigid body placed at the upper end of the column. The direction of the force was kept constant in the numerical analyses, while some variation of the applied load angle,  $q$ , was observed in the experiments due to the test set-up.

The absorbed energy,  $E_a$ , is determined by integration of the force vs. deformation curve. The mean crush load,  $F_{mean}$ , for a given deformation,  $d$ , is defined as the absorbed energy divided by the deformation, see Figure 1. Hence, the mean crush load was used as the response parameter to evaluate the columns' capability of absorbing energy when subjected to oblique loads. The peak force,  $F_{peak}$ , was also used to describe the behavior of the columns.

When a thin-walled column is subjected to pure axial crushing, an initial global peak load is found when the thin-walled elements start to buckle and the first lobe appears. The load values oscillate between local peaks and minimum loads while new lobes are formed, see Figure 2. The columns subjected to oblique loading in this study, however, reached the initial peak load when the first lobe appeared, but after this, the collapse mode switched to global bending, and no more lobes were created.

### 3 Material properties

The aluminum alloy of the square columns was AA6060, temper T4. Although the columns fail by local buckling in the compression flange, standard tensile tests were used to establish the stress–strain curves. This was guided by tests performed by Opheim [4] who found no significant difference in the behavior in tension and compression of the present material. The test specimens were taken out parallel to the extrusion direction. Figure 3 shows a typical engineering stress-strain curve of the alloy used, while Table 1 summarizes the mechanical properties obtained in the material tests.

A proper description of the strain hardening properties of aluminum is necessary for a good correlation between the experimental and predicted responses of the oblique-loaded aluminum extrusions. In the numerical study, the uniaxial true stress-strain behavior was fitted to the constitutive relation:

$$\sigma = \sigma^0 + \sum_{i=1}^2 R_i + \sum_{i=1}^2 X_i + \sigma_v$$

where

$$R_i = \alpha Q_i [1 - \exp(-C_i \varepsilon_p)]$$

$$X_i = (1 - \alpha) Q_i [1 - \exp(-C_i \varepsilon_p)]$$

Here,  $\sigma$  and  $\varepsilon$  is the true stress and strain, respectively.  $\sigma_0$  is the proportionality limit in a uniaxial test,  $\varepsilon_p = \varepsilon - \sigma / E$  is the plastic strain and  $E$  is the elastic modulus.  $C_i$  govern the rate of change in the isotropic and kinematic hardening variables and  $Q_i$  represent their asymptotic values.  $\alpha$  determines the relationship between isotropic and kinematic hardening.  $\sigma_v$  is the viscous stress. As the aluminum alloys are almost strain rate insensitive [5], the viscous effect is neglected in this study. Based on the studies of Langseth et al. [6], the hardening parameter in Equation (1) is taken as  $\alpha = 1.0$ .

The material constants  $\sigma^0$ ,  $C_i$  and  $Q_i$  ( $i = 1, 2$ ) in Table 2 have been determined from the true stress-strain curves for each wall thickness. These curves originate from uniaxial tensile tests using specimens parallel to the extrusion direction.

### 4 Experimental program and test set-up

Energy absorbers are usually subjected to dynamic loads. As dynamic precision tests of oblique loading are quite difficult to accomplish, quasi-static tests have been carried out to validate a numerical model.

Table 3 shows the test specimen's geometry and support conditions. The main objective was to validate a numerical model in order to predict the response of square columns subjected to oblique loading. The length,  $l$ , and width,  $b$ , of the test specimens were constant, 199 mm and 80 mm respectively. Two values of the wall thickness,  $h$ , were used, with average values  $h_1 = 1.9$  mm and  $h_2 = 2.46$  mm. The load angles were  $\theta_1 = 5^\circ$ ,  $\theta_2 = 15^\circ$ , and  $\theta_3 = 30^\circ$ , giving 18 tests with 3 repetitions of each combination of wall thickness and load angle. Peak force and mean crush load were the response parameters. A reasonable displacement to compare mean crush forces was chosen as  $d_{max} = 50$  mm =  $0.25.l$ .

The test specimens were clamped at the lower end and free at the top before applying the load. The wall thickness of the specimens was measured prior to testing, and the variation in thickness relative to the average value was less than 5%. The following identification system was adopted: s $\theta$ -h-n, where s stands for static test,  $\theta$  is the load angle, h the thickness and n is repetition No. n.

### 5 Validation study

Numerical studies were performed using the FE-code LS-DYNA [7]. The main objective was to show that the response of the test specimens could be predicted with sufficient accuracy. In the analyses, focus was placed on the force vs. plastic displacement ( $F$ - $d_p$ ) curves, peak force, energy absorption and collapse modes.

Due to symmetry, one half of the column was modeled using the Belytschko-Tsay shell element. The load was applied at the upper end of the specimen, through a rigid body modeled with shell elements. The free length of the specimens was 199 mm as in the experiments, and the rigid body 70 mm. All the degrees of freedom were fixed at the lower end, while the upper end was fixed to the rigid body. Axial crushing of columns with the same geometry has been studied by Langseth et al. [6], so the number of elements needed were based on these studies, and a total of 5280 elements were used. The element mesh is shown in Figure 4.

To ensure quasi-static loading when using an explicit code, the rigid body was given a prescribed velocity field,  $v(t)$ , following the function

$$v(t) = \frac{\pi}{\pi - 2} \cdot \frac{d_{max}}{T} \left[ 1 - \cos\left(\frac{\pi}{2T} \cdot t\right) \right]$$

Here,  $T$  is the total duration of the loading, and  $d_{max}$  is the final displacement. When integrated from  $t = 0$  to  $t = T$  this expression yields  $d_{max}$ , and when differentiated with respect to time, the initial acceleration equals zero. This ensures that the loading takes place gradually and that unnecessary dynamics in the numerical solution are avoided. An indicator of the dynamics in the system is given by the ratio between static and dynamic loads,  $L(t)$  [8],

$$\frac{F'_s}{F'_d} = L(t) \approx \frac{\Delta E'_s}{\Delta E'_s + \Delta K}$$

where  $\Delta E'_s$  and  $\Delta K$  are the change in internal and kinetic energy, respectively.  $L(t)$  was calculated for all the analyses and was always close to 1.0, which indicates that the analyses were quasi-static.

Initial geometrical imperfections may have an influence on the peak load as well as on the energy absorption, so initial imperfections were prescribed both along the length and width of the model in some of the analyses with following expression:

$$w(x, y) = w_0 \sin\left(\frac{n\pi x}{l}\right) \sin\left(\frac{\pi y}{b-h}\right)$$

Here,  $w_0$  is the amplitude,  $n$  is the number of half-sine waves along the length,  $b$  is the width and  $h$  is the thickness of the section. Based on the studies of Opheim [4], five half-sine waves with amplitude of 0.1, 0.3 and 0.4 mm were applied in some of the numerical simulations. The amplitude  $w_0 = 0.4$  mm represented the manufacturers maximum out-of-flatness allowed for the examined sections. The effect of initial imperfections on peak force and mean force are shown in Figure 5.

One can see that the response parameters are sensitive to the presence of initial imperfections. The peak force varies somewhat for the different amplitudes, but the curve seems to flatten out around the amplitudes of 0.1 mm. The amplitude does not have much influence on the mean force, as long as it is larger than zero. In the numerical analyses that were performed to validate the numerical model, initial imperfections with amplitude  $w_0 = 0.1$  mm were prescribed.

All the columns in the experimental program experienced global bending collapse. The compression flange buckled, and the peak load was then reached followed by a global bending mode giving a plastic hinge close to the clamped support. Three typical bending modes were observed, here called mechanism A, B and C. For mechanism A, the compression flange buckled outward, the webs and tension flange moved inward, see Figure 6. For the columns that experienced mechanism B, the compression flange started to move outwards in the beginning, but the buckle stopped growing. The subsequent deformation of the column was due to a second lobe, see Figure 6. Mechanism C is similar to the hinge mechanism described by Kecman [1] and simply the opposite of mechanism A, as the buckle started moving inward and continued with that.

In the experiments, mechanisms B and C were developed for columns subjected to a load angle of 5 degrees. The columns with load angles of 15 degrees experienced all three modes, while 30 degrees mainly produced mechanism A. One of the repetitions of test s30-2.5 experienced a variant of mechanism B. While the inward buckle of mechanism B usually was much bigger than the outward buckle, the two buckles were about the same size for test s30- 2.5-1.

The numerical analyses without initial imperfections resulted in the same deformation modes as the experiments. Figure 7 shows pictures of mechanism A and B, both from the experiments and the numerical simulations. The analyses are able to predict the global response of the columns, as well as the local mechanism. Force-plastic displacement curves for analyses and all three repetitions from the experiments are given in Figure 8. The results from the analyses are shown for  $w_0 = 0$  mm and  $w_0 = 0.1$  mm. The figure shows that the numerical model was able to describe the force and displacement quite well. While the analyses without initial imperfections overestimated the peak forces and the mean loads, the analyses with initial imperfections gave values very close to the experimental results.

The mean crushing force for an axially loaded column

$$F'_{mean} = 13.06\sigma_0 \cdot h^2 \cdot \left(\frac{b}{h}\right)^{3/2}$$

proposed by Abramowicz and Jones [9] for a rigid plastic material can be calculated for the columns in the experiments. Here, the flow stress,  $\sigma_0$ , is taken as the average value of the yield and ultimate stresses,  $\sigma_{02}$  and  $\sigma_u$  to account for the hardening in the material [10]. The mean axial crushing load is  $F_{mean}$  ( $h=1.9$  mm) = 21.3 kN and  $F_{mean}$  ( $h=2.46$  mm) = 32.8 kN. Figure 9 shows the peak load and the mean load for the experiments and the analyses.  $F_{mean}$  is calculated for a deformation  $d = 50$  mm. The calculated mean crushing force for an axially loaded column is also included in the figure. One can see that the energy absorption ability drops by 50% only by introducing a load angle of  $5^\circ$ . As Figure 9 also shows, the mean load also decrease with increasing load angle, i.e. when introducing bending into the column. The peak load also drops drastically from a load angle of  $5^\circ$  to  $30^\circ$ .

## 6 Conclusions

The crushing behavior of square aluminum columns subjected to oblique loads has been studied, experimentally and numerically, and the following conclusions can be drawn:

- A test rig was built and accurate measurements of the quasi-static response during oblique loading of the aluminum extrusions were obtained.
- The deformation mode seems to depend on both load angle and thickness. The quasi-static simulations were able to predict the local mechanisms that occurred in the experiments.
- LS-DYNA was able to describe the force-plastic displacement curve very well, especially analyses with initial imperfections with amplitudes,  $w_0 = 0.1$  mm gave satisfactory results of mean load and peak force compared to the experiments.
- Analyses without initial imperfections overestimated the peak load. The presence of initial imperfections lowers the peak load considerably. The amplitude seems less important for the mean load, as long as it is larger than zero.
- The energy absorption drops drastically by introducing a load angle of  $5^\circ$  and drops additionally with increasing load angle.

Acknowledgements – The authors would like thank Hydro Automotive Structures for their generous support of the research project that forms the basis for the present work. Thanks are also given to Mr. T. Meltzer, Mr. Lars Olav Jahre and Christian Rykke who has provided technical assistance in the laboratory.

## References

- 1 D. Kecman: *Bending collapse of rectangular and square section tubes*, Int. Journal Mech. Sci. , Vol. 25, No. 9-10, pp.623-636 (1983)
- 2 N. Jones: *Structural Impact*, Cambridge University Press, 1989
- 3 D.C. Han and S.H. Park: *Collapse behavior of square thin-walled columns subjected to oblique loads*, Thin walled structures 35 (1999) 167-184
- 4 B. S. Opheim: *Bending of Thin-Walled Aluminum Extrusions*, Doctoral thesis, Department of Structural Engineering, Norwegian University of Science and Technology. ISBN 82-7119-947-1 (1996)
- 5 M. Langseth, O.G. Lademo: *Tensile and torsion testing of AA6060-T4 and T6 aluminium alloys at various strain rates*, Tech. Report, Department of Structural Engineering, Norwegian University of Science and Technology. (1994)
- 6 M. Langseth, O.S. Hopperstad and T. Berstad: *Crashworthiness of aluminium extrusions: validation of numerical simulation, effect of mass ratio and impact velocity*, Int. Journal of Impact Eng 22 (1999) 829-854
- 7 J. O. Hallquist: *Theoretical Manual*, Livermore Software Technology Corporation, compiled by J. O. Hallquist
- 8 H. Ilstad: *Validation of Numerical Collapse Behaviour of Thin-Walled Corrugated Panels*, Doctoral thesis, Department of Structural Engineering, Norwegian University of Science and Technology. ISBN 82-471-0474-1 (1999)
- 9 W. Abramowicz, N. Jones: *Dynamic progressive buckling of circular and square tubes*, Int. J. Impact Eng., 4(4):243-70 (1986)
- 10 M. Langseth and O.S. Hopperstad: *Static and dynamic axial crushing of square thin-walled aluminium extrusions*, Int. Journal of Impact Eng 18 (1996) 949-968

**Table 1 Mechanical properties (based on the engineering stress-strain curves)**

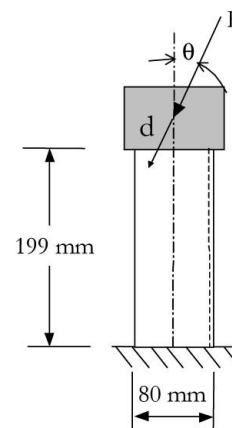
Temper	h [mm]	$\sigma_{0.2}$ [N/mm <sup>2</sup> ]	$\sigma_u$ [N/mm <sup>2</sup> ]	E [N/mm <sup>2</sup> ]
T4	1.90	85	175	66 820
	2.46	82	177	62 766

**Table 2 Material constants for numerical analyses of experiments**

Parameter	h =1.9 mm	h =2.5 mm
$\sigma_0$ [MPa]	68.36	63.35
$C_1$	6913	14410
$Q_1$ [MPa]	13.19	15.88
$C_2$	16.04	14.60
$Q_2$ [MPa]	132	140.8
$\alpha$	1.0	1.0

**Table 3 Test program**

Alloy	Temper	Wall thickness, h [mm]	Angle, $\theta$
AA6060	T4	1.9, 2.5	5
			15
			30



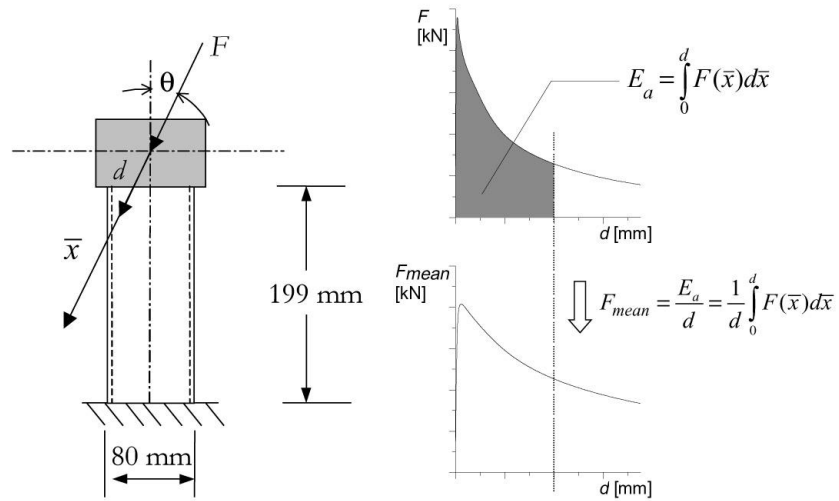


**Figure 1 Oblique loading of column**

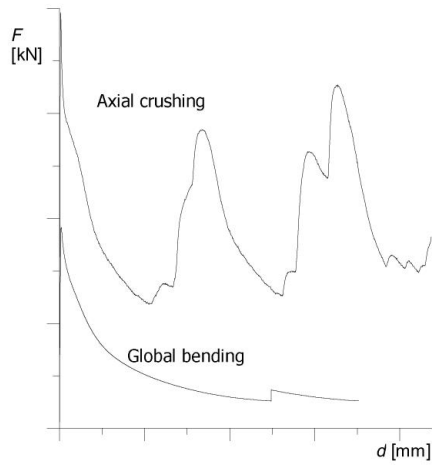


**Figure 2 Typical force - displacement curve for axial crushing and global bending**

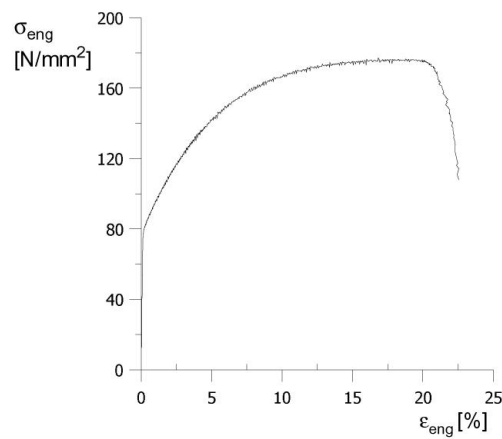


**Figure 3 Typical engineering stress-strain curve**

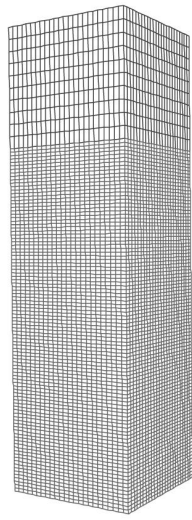


**Figure 4 Finite element model**

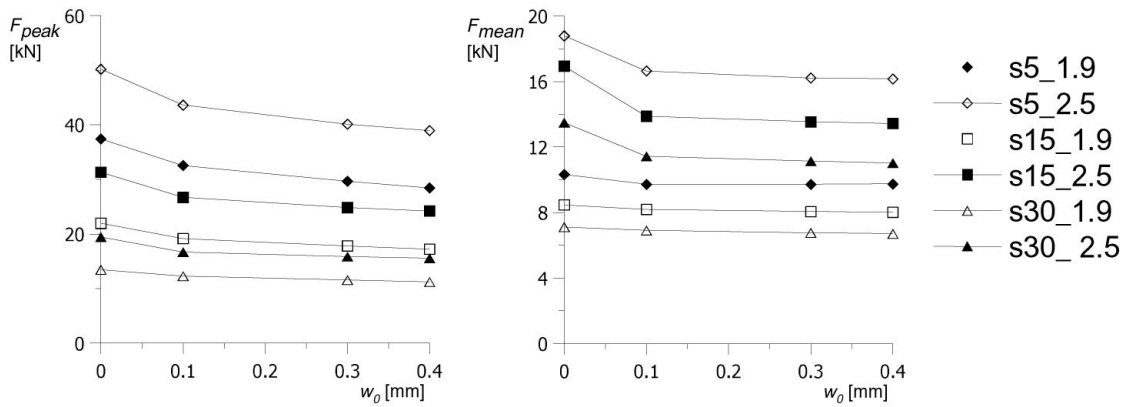


**Figure 5 Peak load and mean load for different amplitudes of the initial imperfections**

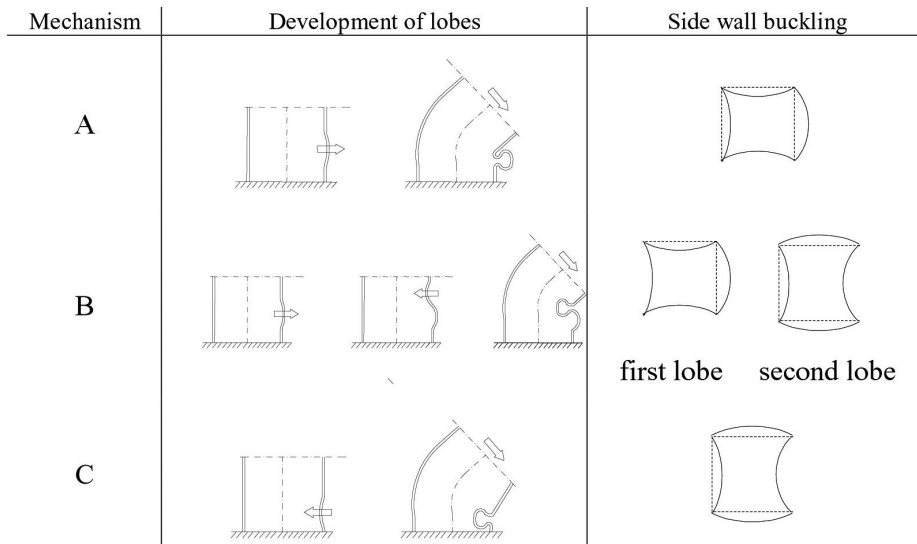


**Figure 6 Deformation modes**

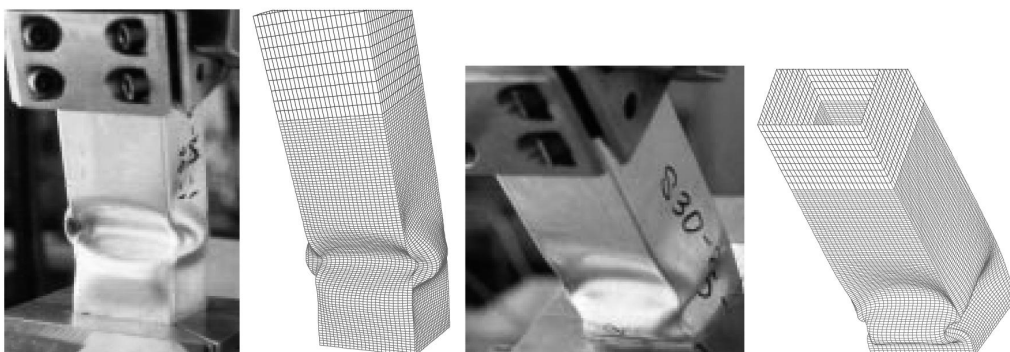


**Figure 7 Pictures from experiments and numerical analyses: s5-2.5 and s30-2.5**

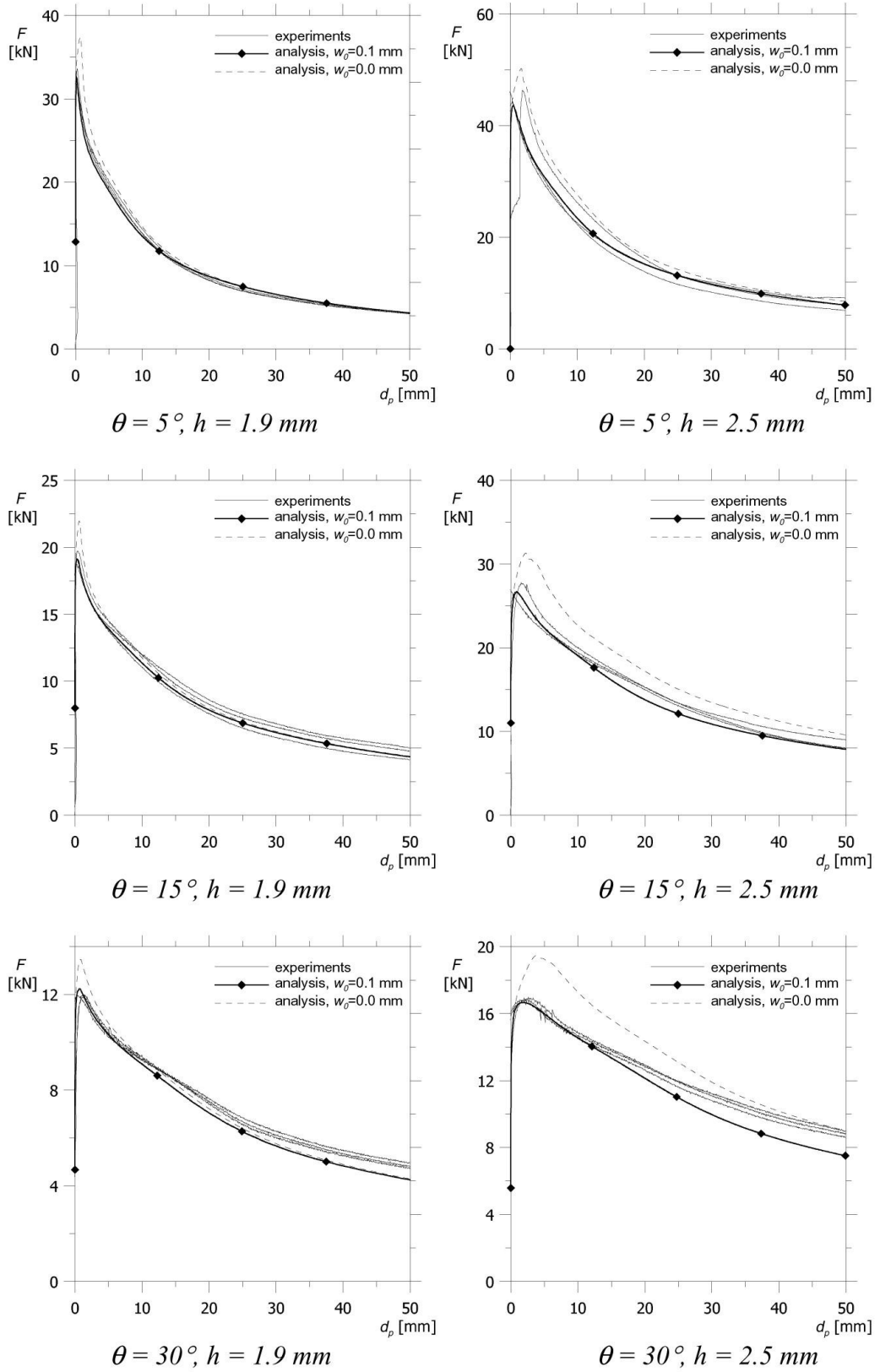


**Figure 8 Applied force vs. plastic displacement.**  
**All three repetitions from the experiments are included.**

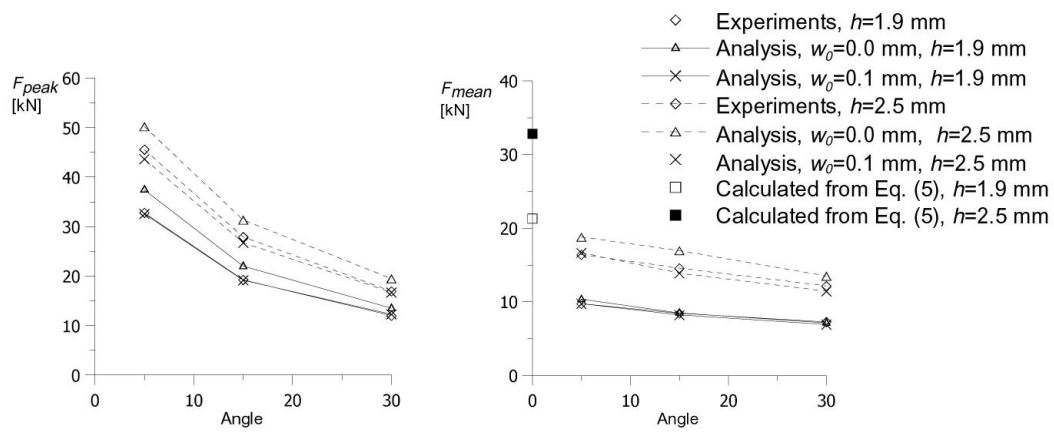


**Figure 9 Peak load and mean load at  $d=50$  mm vs. load angle.  
The calculated mean crushing force for an axially loaded column is also included.**